

## Article

**a special issue** for the scientific conference held by the Department of Chemistry- College of Education for Girls/University of Kufa, under the title:

**(6'th Postgraduate Students Annual Conference ) (PSAC2025).**

which held for Tuesday, **15/4/2025.**

### **Anticancer Activity of Gold (III) Nanoparticles with New Azo Ligand: Synthesis, Characterization and Spectral Identification of Its Metallic Complexes derived from Histidine**

**Rehab Abid Salim<sup>1</sup>, Muna Abass Hadi<sup>1</sup>**

<sup>1</sup> *Department of Chemistry, College of Education for Girls, University of Kufa, AlNahaf, Iraq*

*Email: [rhabbyda@gmail.com](mailto:rhabbyda@gmail.com)*

*Email: [munaa.alsallami@uokufa.edu.iq](mailto:munaa.alsallami@uokufa.edu.iq)*

## Abstract

The new heterocyclic azo ligand, (E)-2-amino-3-(2-((2-hydroxy-4-nitrophenyl)diazenyl)-1H-imidazol-5-yl)propanoic acid, was synthesized by the reaction of histidine with 5-nitro-2-amino phenol. Various analytical methods, including mass spectrometry, <sup>1</sup>H-NMR, FT-IR, CHN elemental analysis, and UV-vis spectroscopy, facilitated the characterization of a recently developed azo ligand. This ligand served as the basis for synthesizing a set of coordination compounds with Ni(II), Cu(II), Co(II), Zn(II), Cd(II), and Au(III) ions, which were subsequently examined using several of the same techniques. Measurements of magnetic susceptibility and molar conductivity were also conducted. The data from electronic spectra and magnetic properties indicate an “octahedral structure” for the entire compounds excluding Au(III) compound, which adopts a “square planar geometry.” All complexes exhibit non-electrolyte properties, with the exception of the Au(III) complex, which displays electrolyte properties. The behavior of the new azo ligand is a tridentate, according to the results overall. The complex Au(III) anticancer properties are very efficacious. The Au-complex destroys leukemia cells while not affecting healthy cells. This compound holds promise as a fresh therapeutic option for

tackling leukemia cancer, with plans brewing to explore its impact on additional cancer varieties down the road.

**Keywords:** *Heterocyclic azo ligand, Histidine, 5-Nitro-2-amino phenol, leukemia*

## Introduction

Azo dyes are compounds of great importance in coordination chemistry due to their ease of preparation, availability, bright colors, and electronic properties[1]. They have also shown importance in the pharmaceutical and analytical fields. Azo compounds containing the (-N = N-) group have gained importance in inorganic chemistry[2]. These compounds are characterized by their ability to react with metal ions to form stable, chelating complexes with five- or six-membered rings [3].

Histidine is an alpha-amino acid with a side chain in the form of a five-membered ring with nitrogen at two side corners. It is classified as a positively charged amino acid because the side chain carries a positive charge on one of the two nitrogen atoms in the ring. This compound contributes to crafting the neurotransmitter histamine by stripping away the carboxyl group from an acid recognized as a vital amino acid for mammals, fish, and poultry, given its absence from internal synthesis and reliance on dietary sources [4-6]. Broad uses unfold across medical realms, pharmaceutical pursuits, and physiological roles [7].

Histidine is the trade name, and the chemical name is 2-amino-3-(1H-imidazole-4-yl) propanoic acid. The formula weight of histidine (C<sub>3</sub>H<sub>9</sub>N<sub>3</sub>O<sub>2</sub>) is approximately 155.16 g/mole. Figure 1 displays the histidine structure.

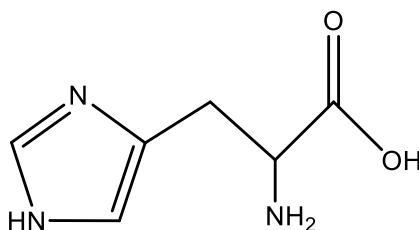


**Figure.1. Histidine structure.**

L-histidine stands as an essential amino acid, vital for building proteins and tackling numerous tasks within cells and tissues. Serving as the starting point for histamine offers a clear instance of this role. Over three decades, curiosity has swirled around simple and complex 2-alkylhistamines, eyed as possible histamine agonists and/or antagonists [8].

Histidine ranks among the 22 proteinogenic amino acids. From a nutritional standpoint, infancy marks histidine as an essential amino acid for humans; maturity shifts this status as synthesis kicks in, rendering it a non-essential amino acid [9, 10]. In our study, we demonstrate the synthesis, characterization, and evaluation of the

anticancer activity of the new azo by reacting histidine with 5-nitro-2-aminophenol and determining its acute toxicity.

## **EXPERIMENTAL SECTION**

### **Materials**

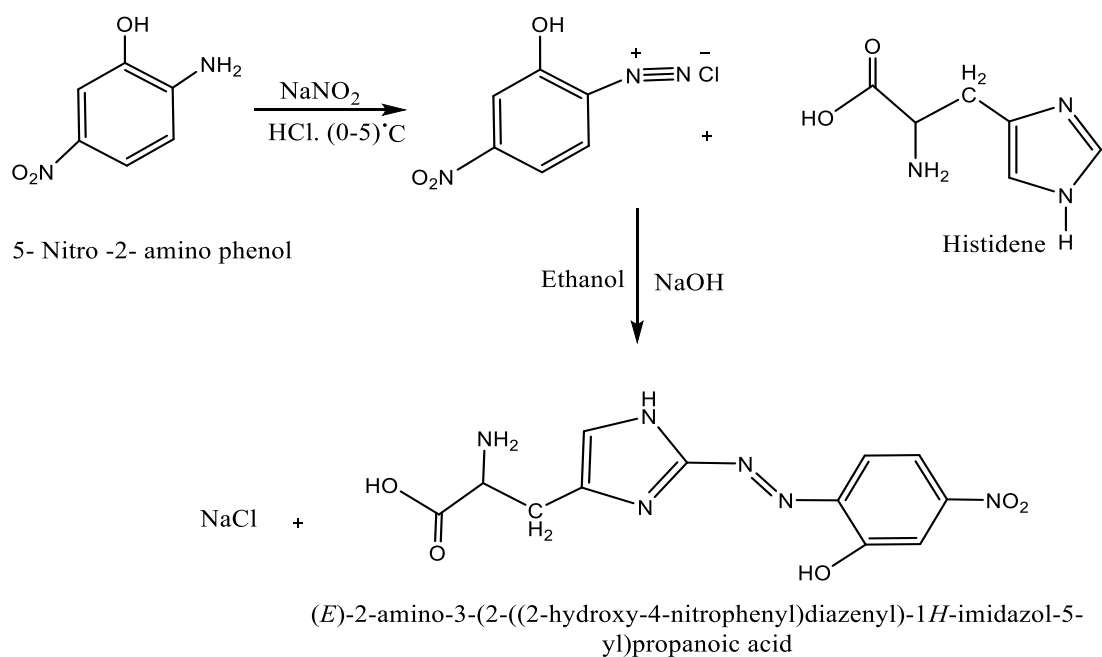
Measuring the melting point of the ligand and its complexes relied on the electrothermal melting point model 9300. A microanalytical unit, the 1180 (CHN) elemental analyzer, handled the task of performing elemental analyses.

A Shimadzu double-beam UV-Vis spectrophotometer (1700) measured electronic absorption spectra. FTIR spectra were obtained in the form of KBr discs with a Shimadzu FTIR spectrophotometer (8400) covering the range of 4000 to 400  $\text{cm}^{-1}$ . The  $^1\text{H-NMR}$  spectra, expressed in parts per million (ppm), were acquired in  $\text{DMSO-d}_6$  solvent utilizing a "Bruker-Ultra Shield" 3000MHz instrument from Switzerland. Magnetic susceptibility measurements were conducted using an MSB-MKI magnetic balance, employing the Faraday technique. Corrections for diamagnetic contributions were performed using Pascal's constants.

### **Procedure**

#### **Synthesizing New Azo Ligand (HL)**

A new azo ligand (HL) was prepared by coupling a diazonium salt solution by dissolving 1.54 g (0.01 mol) of 5-nitro-2-aminophenol in 80 ml of deionized water and 2 ml of strong hydrochloric acid (37%) with continuous shaking. The solution was then cooled to 0-5  $^{\circ}\text{C}$ , and  $\text{NaNO}_2$  solution (0.01 mol, 0.7 g) was added to 10 mL of water. Afterward, the solution was left for 20 minutes in an ice bath. This diazo solution was added dropwise to (0.01mol, 1.55 g) of histidine (the coupling compound) dissolved in 50 mL of ethanol and 50 ml of 10% NaOH solution, where the solution's color was observed to be dark red. The reacting mixture was left for the next day, after which dilute hydrochloric acid was added dropwise to adjust the hydrogen ion concentration (pH) to reach 7. A red precipitate was observed to form. It was filtered and washed many times by distilled water to remove the sodium chloride salt from the chemical chain reaction. It was then recrystallized from ethanol and dried at 60 $^{\circ}\text{C}$  in an oven. Its melting point was measured at 250-251 $^{\circ}\text{C}$ . The procedures for preparing the new azo ligand are shown in scheme 1.



**Scheme 1. Synthesizing new azo ligand derived from histidine**

### Synthesizing Metal Complexes

Chelate complexes of the newly synthesized new azo ligand with Cd(II), Co(II), Zn(II), Cu(II), and Ni(II) ions were prepared in the solid state using a general method, applying a (1:2) molar ratio of metal to ligand (M:L). In contrast, a (1:1) molar ratio was employed for the Au(III) complex. The procedure involved dissolving the appropriate amounts of each metal salt in 30 ml of distilled water and combining them with a ligand solution (0.002 mol, 0.320 g) previously dissolved in ethanol (30 ml). After adding 0.5 ml of ammonium hydroxide, the blend was heated for one hour, during which the formation of colored complexes was visually confirmed. The solution was allowed to stand, forming a precipitate that was subsequently dried and purified through recrystallization utilizing hot absolute ethanol. The resulting pure solids were isolated, and the synthesized metal complexes' melting points were determined. Details of the obtained complexes are presented in Table 1.

### Methods Cell Lines and Culture

K562 (human myeloid leukemia cell line) and HUVEC (normal human fibroblast cell line) were obtained from the "National Cell Bank of Iran (Pasteur Institute, Iran)". Cultivation was carried out in RPMI-1640 and DMEM-F12 media (Gibco), respectively, each supplemented with 10% fetal bovine serum (FBS; Gibco) and antibiotics, including penicillin (100 U/ml) and streptomycin (100 µg/ml). Cell cultures were incubated at 37 °C in a humidified atmosphere with 5% CO<sub>2</sub> and

subcultured utilizing trypsin EDTA Gibco along with PBS (phosphate-buffered saline) solution.

### **MTT Cell Viability Assay**

Cell proliferation and viability were assessed using the MTT “[3-(4,5-dimethylthiazol-2-yl)-2,5-diphenyltetrazolium bromide]” (Sigma-Aldrich) assay. In summary, cells were enzymatically detached using trypsin, collected, and adjusted to a concentration of  $1.4 \times 10^4$  cells per well. The cell suspension was then distributed into 96-well plates, each containing 200  $\mu$ l of fresh culture medium, and incubated for 24 hours. Upon reaching monolayer confluence, treatment was applied using C1 and C2 compounds at concentrations ranging from 600 to 7.4  $\mu$ g/ml for a duration of 24 hours at 37 °C in a 5% CO<sub>2</sub> atmosphere. Following the 24-hour treatment period, the monolayer culture remained undisturbed in the original plate while the supernatant was carefully discarded. Following this step, each well received 200  $\mu$ l of MTT solution (0.5 mg/ml prepared in phosphate-buffered saline (PBS)). The plate underwent incubation at 37 °C for a further 4 hours. Upon completion, the supernatant containing MTT was carefully discarded, and 100  $\mu$ l of dimethyl sulfoxide was introduced into each well. The plate was then placed on a shaker at 37 °C to ensure complete dissolution of the formazan crystals. Absorbance was subsequently measured at 570 nm using an ELISA reader (Model Wave XS2, BioTek, USA) to determine cell viability. The half-maximal inhibitory concentration (IC<sub>50</sub>), indicating the compound concentration required to induce 50% cell mortality, was calculated based on the corresponding dose-response curves.

### **Results and Discussion**

All synthesized complexes exhibited complete solubility in DMSO, DMF, ethanol, and methanol and displayed stability when exposed to air. Characterization of the metal complexes was performed using element analysis, FT-IR, magnetic susceptibility, <sup>1</sup>H-NMR spectra, mass spectrometry, UV-Vis spectroscopy, and molar conductivity measurements. Examination of the complexes’ analytical data aligns closely with findings from hands-on experiments. Numbers indicate a metal-to-ligand balance of (1:2). However, the Au(III) complex stands apart at (1:1). The octahedral shape was confirmed by room temperature measurements of the chelate complexes’ magnetic susceptibility. Yet, the Au(III) complex hinted at a square planar arrangement surrounding the core metal ion. Testing revealed non-conductivity across all crafted chelate complexes in this study, save for the Au(III) complex, which displayed conductivity values in solvent (DMSO).

**Micro analysis:**

Detailed elemental analysis of complexes exhibiting a 1:2 (M:L) ratio demonstrated strong concordance between theoretical predictions and experimental outcomes, as presented in Table 1. The newly synthesized new azo ligand's purity was evaluated using CHN analysis and the TLC technique.

**Table 1. Element analysis of new azo ligand and metal complexes**

Compounds	MWt	Color	Melting Point	%Yield	Found (Calc)%			
					C	H	N	M
C <sub>12</sub> H <sub>12</sub> N <sub>6</sub> O <sub>5</sub>	320	Drak red	250-251 <sup>0</sup> C	86	(45.00) 45.78	(3.75) 3.78	(26.25) 26.24	----
[Co(C <sub>12</sub> H <sub>11</sub> N <sub>6</sub> O <sub>5</sub> ) <sub>2</sub> ].H <sub>2</sub> O	714.9	Drak green	185-187 <sup>0</sup> C	85	(40.28) 40.65	(3.07) 3.75	(23.49) 23.45	(8.23) 8.84
[Ni (C <sub>12</sub> H <sub>11</sub> N <sub>6</sub> O <sub>5</sub> ) <sub>2</sub> ].H <sub>2</sub> O	714.6	Purple	215-217 <sup>0</sup> C	80	(40.30) 40.67	(3.07) 3.63	(23.50) 23.76	(8.19) 8.46
[Cu (C <sub>12</sub> H <sub>11</sub> N <sub>6</sub> O <sub>5</sub> ) <sub>2</sub> ]	701.5	Green	244-246 <sup>0</sup> C	84	(41.05) 41.87	(3.13) 3.28	(23.94) 23.53	(9.05) 8.03
[Zn (C <sub>12</sub> H <sub>11</sub> N <sub>6</sub> O <sub>5</sub> ) <sub>2</sub> ]	703	Purple	282-284 <sup>0</sup> C	76	(40.96) 40.98	(3.12) 3.86	(23.89) 23.93	(9.24) 8.34
[Cd(C <sub>12</sub> H <sub>11</sub> N <sub>6</sub> O <sub>5</sub> ) <sub>2</sub> ]	750	Purple	256-257 <sup>0</sup> C	83	(38.4) 38.65	(2.93) 2.65	(22.4) 22.94	(14.98) 14.56
[Au(C <sub>12</sub> H <sub>11</sub> N <sub>6</sub> O <sub>5</sub> )Cl]Cl	587	Brown	310 <sup>0</sup> C Dec.	78	(24.53) 24.76	(1.87) 1.98	(14.31) 14.87	(33.56) 34.78

**Infrared spectra**

The infrared spectra of both the synthesized complexes and the free azo ligand are presented in Table 2, which compiles the complete set of spectral data. In the spectra of uncoordinated ligand, broad absorption bands appearing in the range of 3600–2400 cm<sup>-1</sup>, corresponding to the stretching vibrations of  $\nu(\text{COOH})$ ,  $\nu(\text{NH}_2)$ ,  $\nu(\text{NH})$  associated with histidine, and  $\nu(\text{OH})$  of 5-nitro-2-amino-phenol [11,12]. The absorption band observed at 1581 cm<sup>-1</sup>, attributed to the azomethine (C=N) group within the imidazole ring of the azo ligand, experiences a shift to a lower frequency upon complexation.

This observation confirms the involvement of the nitrogen atom from the azomethine group in the coordination process [13]. Additionally, the spectrum of the free azo ligand displays a characteristic band at 1498 cm<sup>-1</sup>, corresponding to the N=N functional group. In the metal complexes, this band shifts to a lower frequency, reinforcing the evidence of the azo nitrogen atom's role in metal coordination [14, 15]. Broad absorption bands in the infrared spectra of the Co(II) and Ni(II)

complexes signified the existence of water molecules. In addition, all synthesized complexes exhibited distinct new bands within the ranges of  $503\text{--}545\text{ cm}^{-1}$  and  $428\text{--}474\text{ cm}^{-1}$ , corresponding to the stretching vibrations of  $\nu(\text{M--N})$  and  $\nu(\text{M--O})$ , respectively. These spectral features confirmed the involvement of both nitrogen and oxygen donor atoms from the ligand in coordination with the metal ions [16,17]. The spectral profiles for the newly synthesized azo ligand and the Cu(II) complex are illustrated in Figures 2 and 3.

**Table 2. FTIR of new azo ligands**

Formula	$\nu(\text{COOH})$ $\text{H}_2\text{O}$	$\nu(\text{NH})$ amide	$\nu(\text{C=N})$ imidaz	$\nu(\text{N=N})$	$\nu(\text{M-N})$	$\nu(\text{M-O})$
$\text{C}_{12}\text{H}_{12}\text{N}_6\text{O}_5$	2400-3600	3442	1581	1498,1460	-----	-----
$[\text{Co}(\text{C}_{12}\text{H}_{11}\text{N}_6\text{O}_5)_2]\cdot\text{H}_2\text{O}$	2400-3600	3358	1521	1406	518	474
$[\text{Ni}(\text{C}_{12}\text{H}_{11}\text{N}_6\text{O}_5)_2]\cdot\text{H}_2\text{O}$	2500-3600	3361	1521	1408	545	430
$[\text{Cu}(\text{C}_{12}\text{H}_{11}\text{N}_6\text{O}_5)_2]$	2400-3600	3352	1514	1450,1409	543	428
$[\text{Zn}(\text{C}_{12}\text{H}_{11}\text{N}_6\text{O}_5)_2]$	2500-3600	3332	1517	1404	503	462
$[\text{Cd}(\text{C}_{12}\text{H}_{11}\text{N}_6\text{O}_5)_2]$	2400-3600	3346	1521	1413	524	474
$[\text{Au}(\text{C}_{12}\text{H}_{11}\text{N}_6\text{O}_5)\text{Cl}]\text{Cl}$	3500	3446	1523	1404	542	430

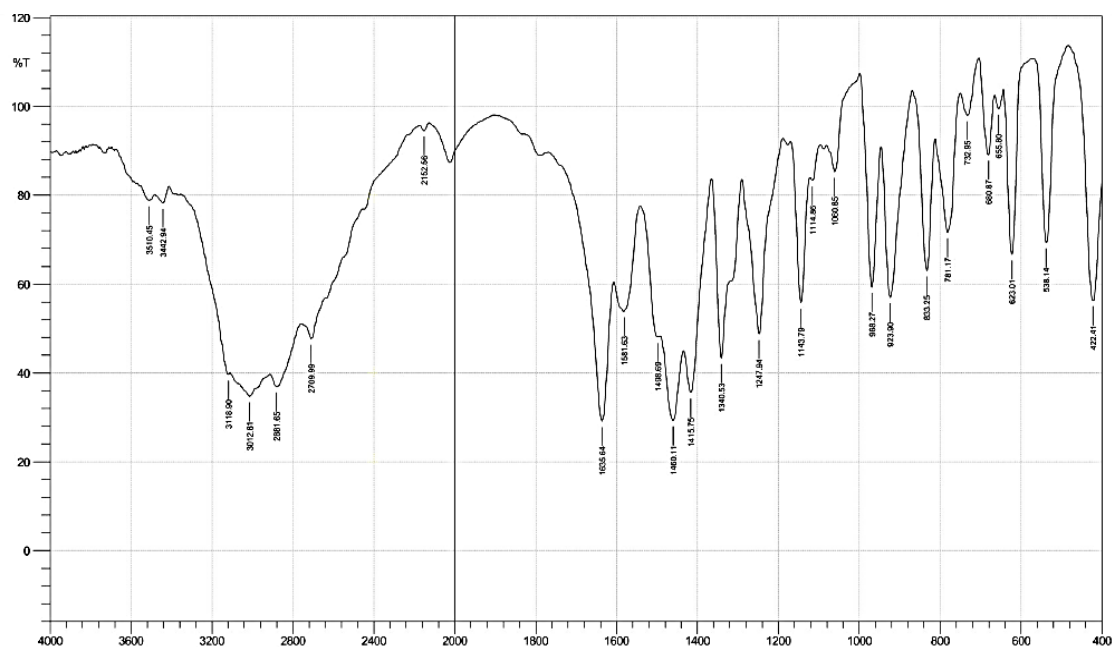


**Fig. 2. New Azo ligand FTIR**

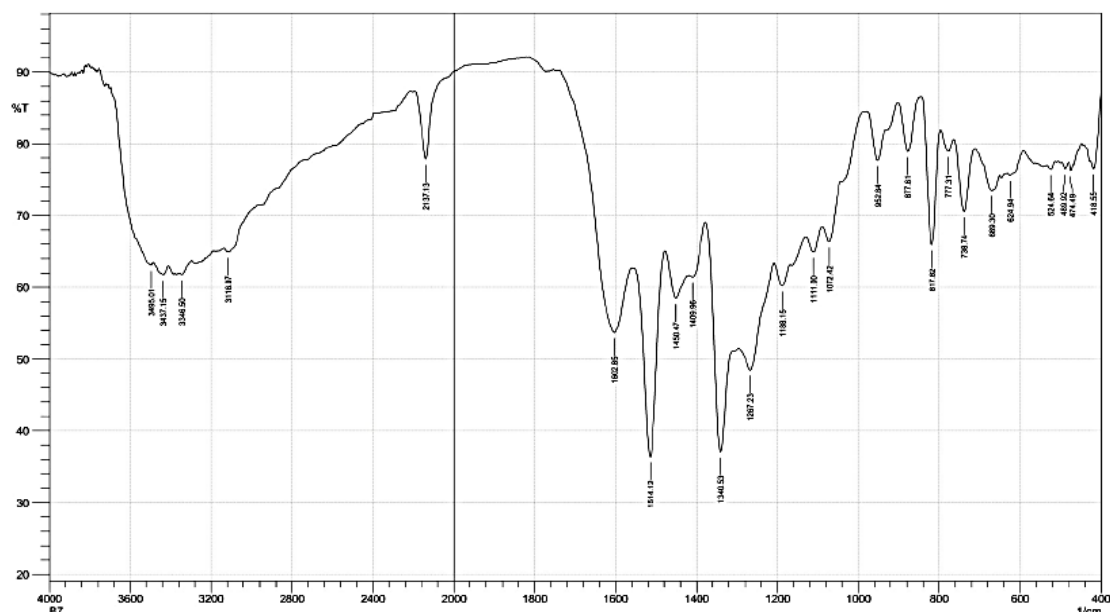


**Fig. 3.** Cu (II) complex FTIR

### Electronic spectroscopy

Electronic spectroscopy is a key technique in coordination chemistry. It involves analyzing the spectra of metal complexes and comparing them with the spectrum of the free ligand. The electronic absorption spectrum of the newly synthesized azo ligand shows two charge transfer (CT) bands: one at 276 nm ( $36231\text{ cm}^{-1}$ ) and another at 347 nm ( $28818\text{ cm}^{-1}$ ). These bands are assigned to  $\pi\text{-}\pi^*$  and  $n\text{-}\pi^*$  transitions throughout the azo ligand.

The peak observed at 347 nm within the spectrum of the unbound ligand moves to an extended wavelength span of 384–585 nm when examining the metal complexes, suggesting a ligand-to-metal charge transfer (LMCT) transition [18, 19]. This alteration hints at an octahedral arrangement encircling the metal(II) ions across most complexes, whereas the Au(III) complex reveals a square planar structure. Figure 4 displays the UV-Vis spectra for both the recently developed azo ligand and the Co(II) complex, offering a clear view of these spectral shifts.

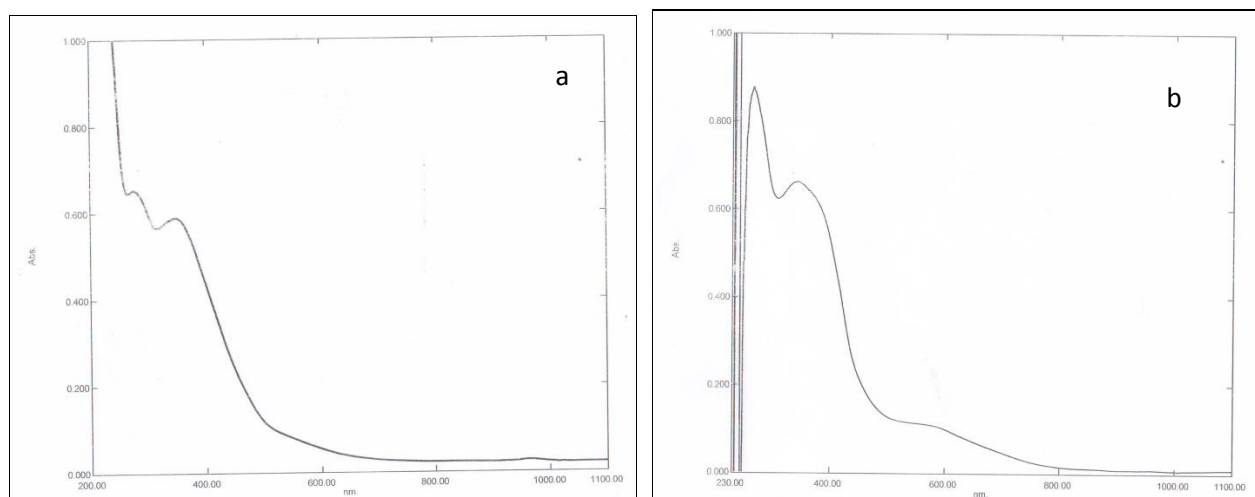
### Measurement of conductivity

Table 3 displays the measured conductivity values ( $\Lambda\mu$ ) for the synthesized metal complexes, determined in dimethyl sulfoxide (DMSO) at a molar concentration of  $10^{-3}\text{ M}$ , with all measurements conducted at room temperature. The obtained chelate complexes exhibited conductivity values ranging from 10 to  $18\text{ S}\cdot\text{cm}^2\cdot\text{mol}^{-1}$ , which signifies their classification as non-electrolytes [20]. The Au(III) complex exhibited a molar conductance of  $33\text{ S}\cdot\text{cm}^2\cdot\text{mol}^{-1}$ , which corresponds to an electrolyte nature, specifically with a 1:1 electrolyte ratio [21]. Based on this

observation, the likely structural arrangements of the metal complexes are illustrated in Fig. 13.

**Table 3. Spectral, structural, magnetic, and conductivity data**

Formula	$\lambda_{\max}$ (nm)	Absorption Bands ( $\text{cm}^{-1}$ )	Transitions	$\mu_{\text{eff}}$ (B.M)	Geometry	Hybridization	Conductivity $\text{S.mol}^{-1} \cdot \text{cm}^2$
HL= $\text{C}_{12}\text{H}_{12}\text{N}_6\text{O}_5$	276 347	36231 28818	$\pi \rightarrow \pi^*$ $n \rightarrow \pi^*$	----	----	----	---
$[\text{Co}(\text{C}_{12}\text{H}_{11}\text{N}_6\text{O}_5)_2] \cdot \text{H}_2\text{O}$	585	17094	MLCT	3.1	Octahedral	$\text{Sp}^3\text{d}^2$	18
$[\text{Ni}(\text{C}_{12}\text{H}_{11}\text{N}_6\text{O}_5)_2] \cdot \text{H}_2\text{O}$	545	18348	MLCT	2.3	Octahedral	$\text{Sp}^3\text{d}^2$	10
$[\text{Cu}(\text{C}_{12}\text{H}_{11}\text{N}_6\text{O}_5)_2]$	547	18281	MLCT	1.7	Octahedral	$\text{Sp}^3\text{d}^2$	12
$[\text{Zn}(\text{C}_{12}\text{H}_{11}\text{N}_6\text{O}_5)_2]$	527	18975	MLCT	Dia	Octahedral	$\text{Sp}^3\text{d}^2$	17
$[\text{Cd}(\text{C}_{12}\text{H}_{11}\text{N}_6\text{O}_5)_2]$	530	18867	MLCT	Dia	Octahedral	$\text{Sp}^3\text{d}^2$	17
$[\text{Au}(\text{C}_{12}\text{H}_{11}\text{N}_6\text{O}_5)\text{Cl}]\text{Cl}$	384	26041	MLCT	Dia	square planar	$\text{dsp}^2$	33



**Fig. 4. UV-Vis spectra of azo ligand and Co(II) complex**

### Mass spectra

The mass spectra of the synthesized ligands and the Au(III) complexes are presented in (Figs. 5 and 6). The mass spectrum of the new azo ligand reveals a prominent base peak at  $M/Z^+ = 320$ , corresponding to the molecular ion peak, thereby supporting the proposed molecular structure. The spectra of the Au(III) complex displayed a molecular ion peak on  $M/Z^+ = 587$ , aligning well with the molecular formula proposed based on microanalytical results.

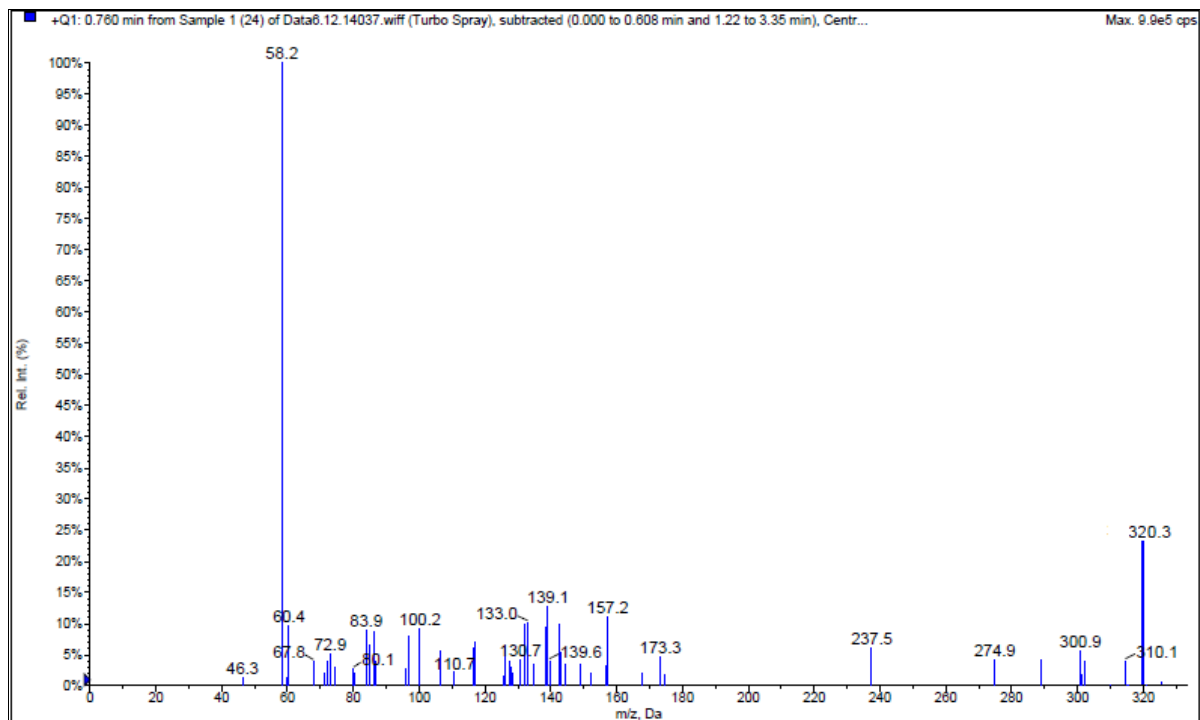


Fig. 5. Spectrum of new azo ligand

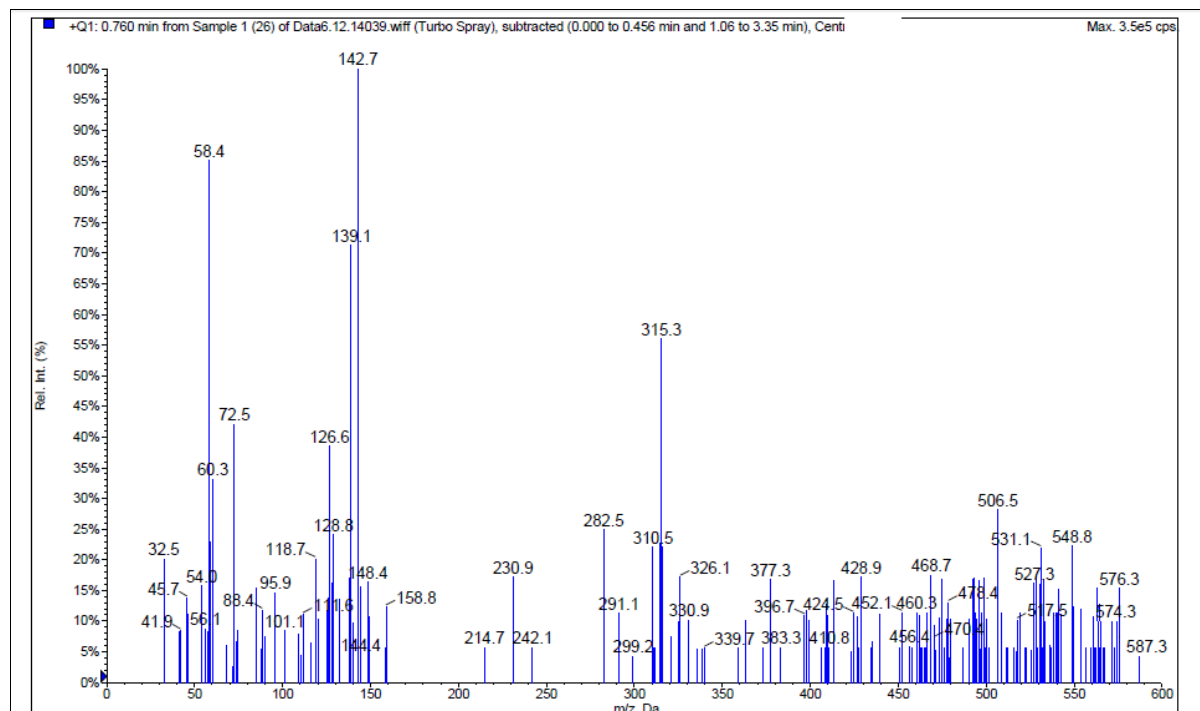
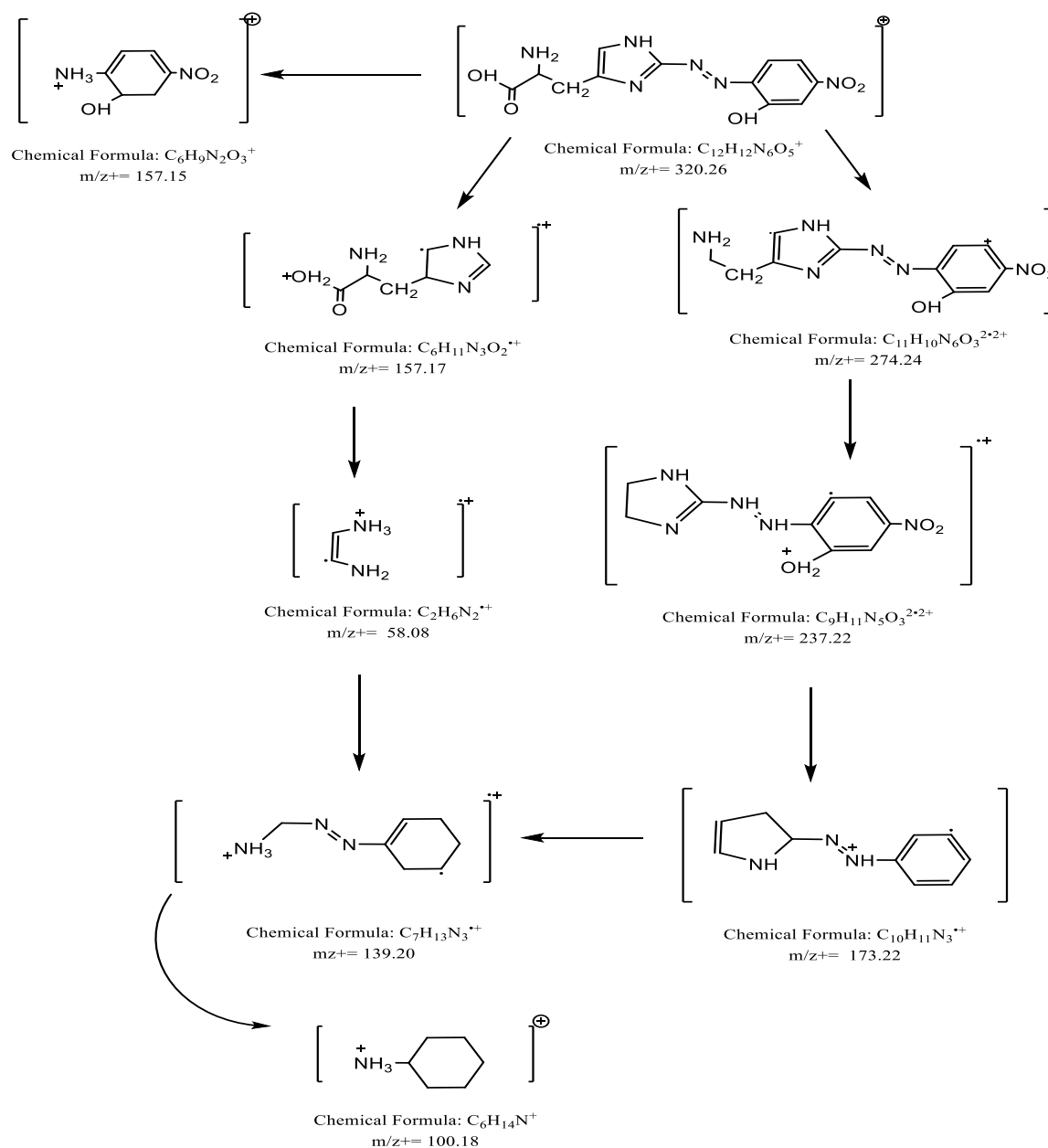


Fig. 6. Spectrum of Au(III) complex



Scheme 2. Fragment of the new Azo ligand

### $^1\text{H-NMR}$ spectra

Figures 7 and 8 present the  $^1\text{H-NMR}$  spectral data of the newly synthesized azo ligand and the Zn(II) complex, recorded in  $\text{DMSO-d}^6$  using TMS as the internal standard. Within the ligand's  $^1\text{H-NMR}$  spectrum, a singlet signal observed at  $\delta 2.5\text{ppm}$  corresponds to protons originating from the solvent. The aromatic protons appeared as multiple signals in the range of  $\delta$  (7.0-8.0) ppm, showing Carboxylic acid (COOH) signal at 12.5 ppm, a signal at  $\delta$  3.5 ppm was observed for the (-CH-) proton in the imidazole ring, while another signal at  $\delta 12.7\text{ppm}$  was assigned to the imidazole (-NH-) proton [22]. The signal of the Phenolic-OH group at 10.9 ppm,  $\text{CH}_2$  at 2.6 ppm, and signal (4.8) ppm belong to the  $\text{NH}_2$  group. In the spectrum of the Zn(II)

complex, the absence of the phenolic –OH proton signal suggests the involvement of the oxygen atom in coordination [23]. All other proton signals in the complex remain essentially unchanged.

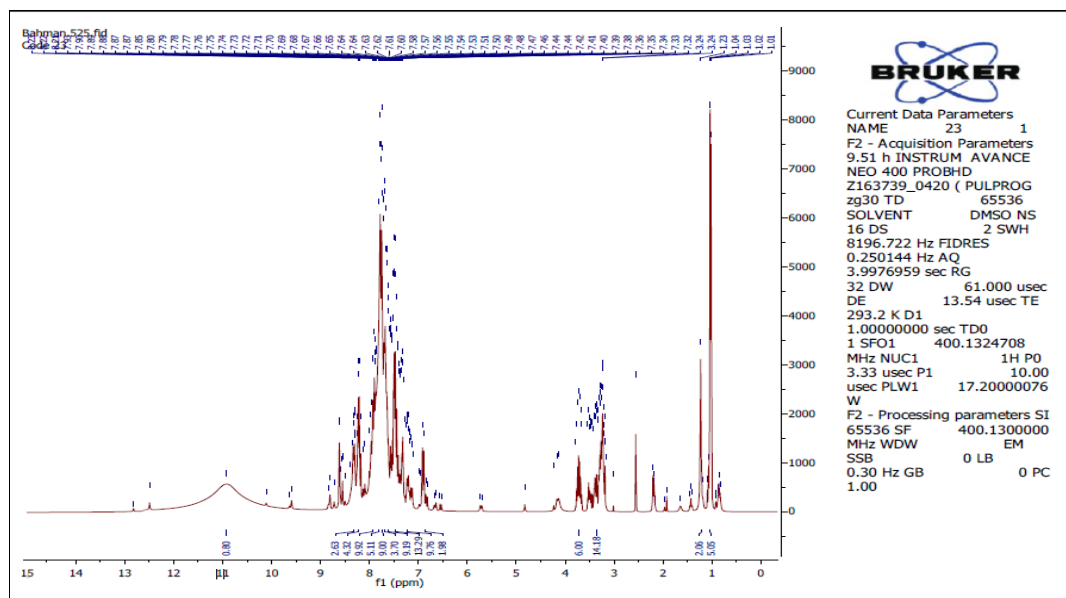


Fig. 7. <sup>1</sup>H-NMR Spectrum of New azo ligand

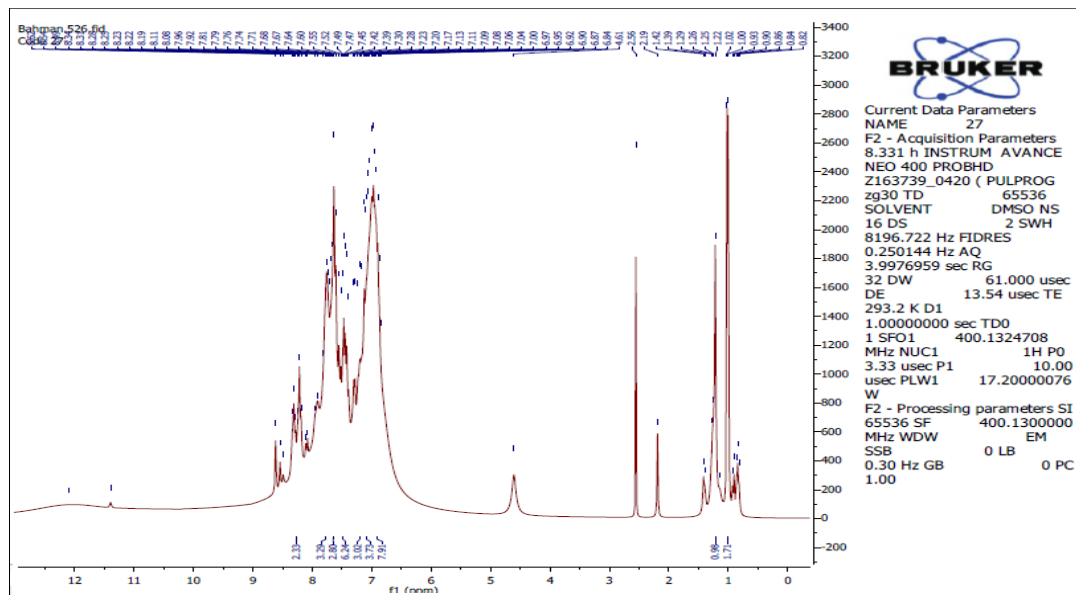


Fig. 8. <sup>1</sup>H-NMR Spectrum of Zn(II) complex.

## Anticancer activity of Au(III) complex

The potential application of the newly synthesized complexes in cancer treatment was explored through biological evaluation. In this investigation, the antitumor properties of the prepared compounds, including the Au(III) complex, were assessed using the human myeloid leukemia K562 cell line. Among the tested compounds, the Au(III) complex exhibited the most significant inhibitory effect, with an  $IC_{50}$  value recorded at 57.87  $\mu\text{g/mL}$  [24].

The cytotoxic impact of the examined Au(III) complex on cells was determined through quantitative analysis. Cell viability was assessed by measuring optical density using a microplate reader, enabling the estimation of living cell numbers. The percentage of viable cells was then calculated according to the following formula:

$$\text{Cytotoxicity} = \frac{A-B}{A} \times 100 \quad \text{Eq. (1)}$$

In which:

A, B are control and test's optical density.

The correlation between cell viability and concentration of compound was illustrated through survival curves generated for each tumor cell line following exposure to the tested substances. The cytotoxic performance of the Au(III) complex was specifically evaluated against the human myeloid leukemia K562 cell line at varying concentration levels.

**Table 4: Au(III) complex inhibition percentage**

Con.( $\mu\text{g/mL}$ )	Mean percentage for every cell line			
	K562		HUVEC	
	Cancerous line cells of K562		Normal line cells of HUVEC	
	Cell Viability	Cell Inhibition	Cell Viability	Cell Inhibition
7.4	88.68	11.32	92.04	7.96
22.22	82.47	17.53	83.78	16.22
66.66	33.33	66.67	71.02	28.98
200	18.88	81.12	26.43	73.57
600	12.73	87.27	21.33	78.67

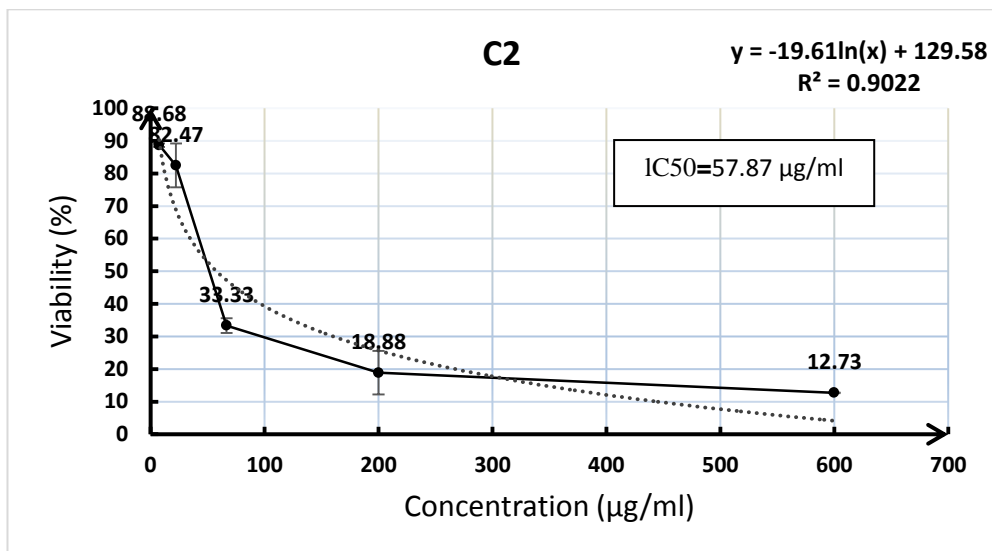


Fig.9: Curve with plotting of IC50 of Au(III) complex for K562.

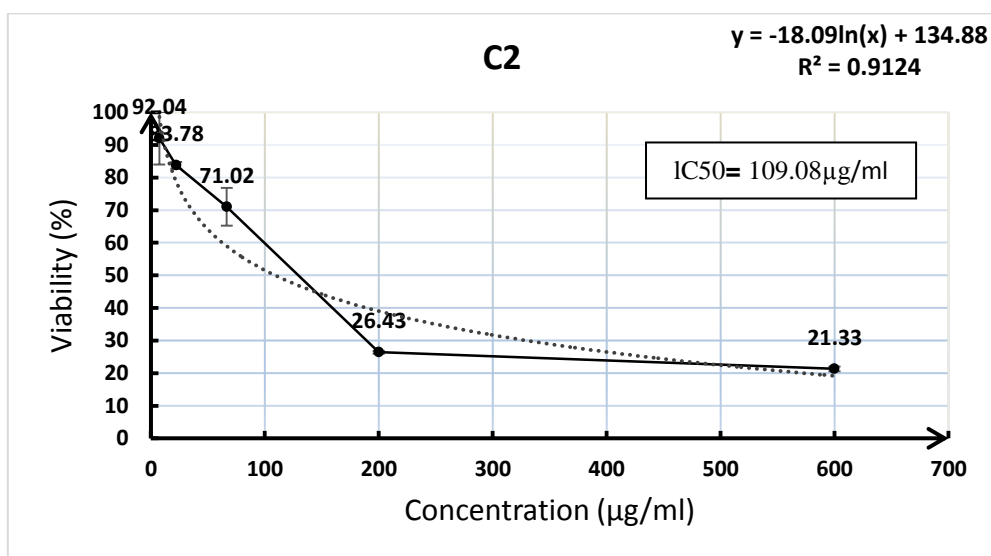
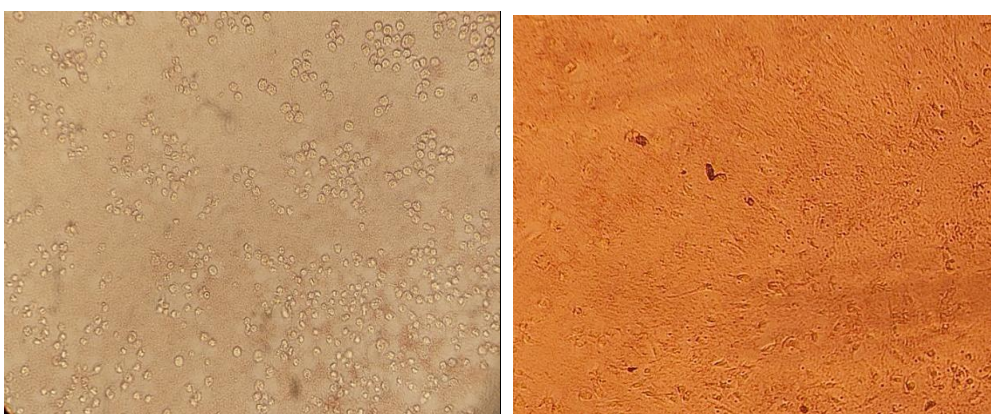


Fig.10: Curve with plotting of IC50 of Au(III) complex for HUVEC.



Au(III) complex for K562

Au(III) complex for HUVEC

Fig. 11. Inhibition in cells K562 and HUVEC of Au(III) complex

## FESEM

The FESEM was employed to examine the crystal structure concerning the morphology and dimensions of the particles, as well as the dispersion of the nanoparticle crystals. The microscope was used to capture images of the crystals of the Au(III) trivalent complexes with a new azo ligand, showing that the complex particles are spherical. The average particle size was 127nm, the complication period using the reflex method was 2 hours, and a temperature of 80°C. Under identical experimental conditions, extending the preparation time to 25 hours resulted in a notable transformation in the morphology of the complex particles, shifting from a spherical form to nanoscale sheets with an average size of approximately 45 nm. This morphological evolution suggests that prolonging the synthesis duration facilitates the assembly of complex nanoparticles into less uniform, sheet-like nanostructures [25].

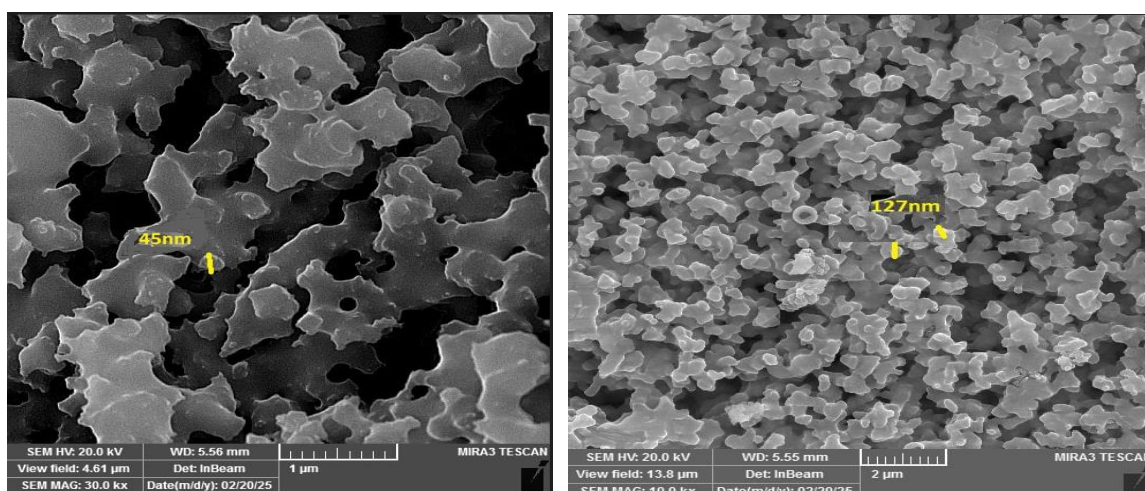


**Fig.12. FE-SEM images of Au(III) metal complexes.**

## Metal Complexes' Suggested Structures

Based on the results obtained from analytical measurements and spectroscopic techniques, as illustrated in Fig.13, the newly synthesized azo ligand functions as a tridentate chelating agent. Coordination occurs through the nitrogen atoms present in the (N=N) azo group and the azomethine moiety of the imidazole ring found in the histidine derivative, along with the oxygen atom belonging to 5-nitro-2-aminophenol.

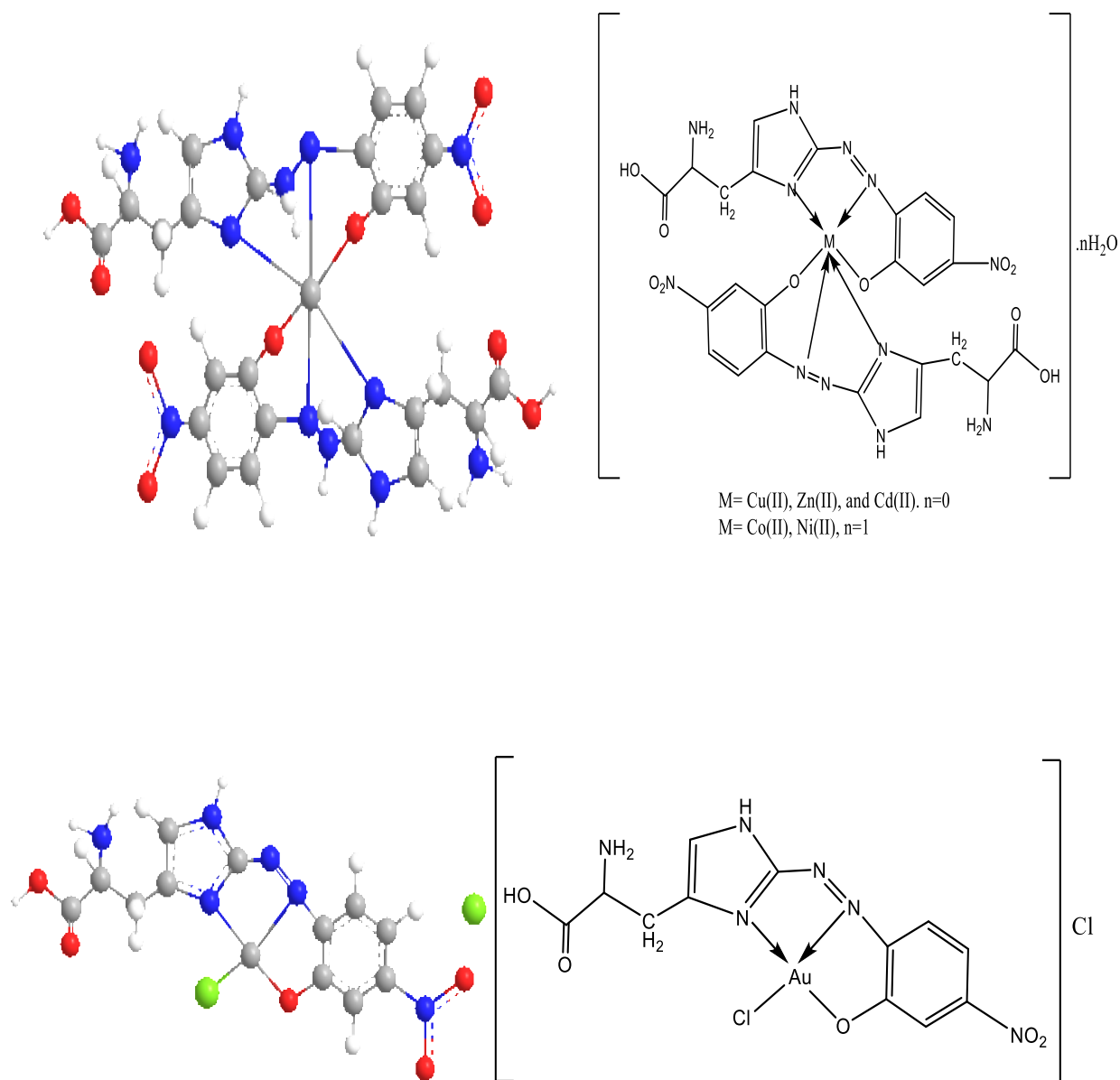


**Fig.13. The proposed structural formula of the complexes.**

## Conclusions

This study presents the preparation and characterization of a novel set of cobalt(II), zinc(II), copper(II), nickel(II), gold(III), and cadmium(II) complexes formed with a newly synthesized heterocyclic azo ligand derived from histidine. A range of physicochemical analytical methods was employed to investigate these chelate complexes. Spectral analyses confirmed that the ligand acts as a neutral tridentate donor, coordinating through three distinct donor sites to the metal centers. The spectral and magnetic studies of the prepared metal complexes of the new azo ligand reveal that all ligand chelate complexes have octahedral geometry except the Au(III) complex, which suggests a square planar geometry around the central metal ion. Also, from the current investigation, It may be inferred that the ligand and

Au(III) complex preparation have appeared in a human myeloid leukemia K562 cell line, in addition to the gold complex having nanoparticle crystal properties through the results.

## **Reference**

- [1] Sayqal A, Alotaibi M M, Kassem M A, & S A Ahmed [2024]: Competence azo dyes sensors of new based fluorophores for spectrophotometric trace determination of cobalt in real water samples. *Arabian Journal of Chemistry*, 17(4), p. 105686.
- [2] Shalabi K, El-Lateef H M A, Hammouda M M, & Abdelhamid A A. [2024]: Green Synthesizing and Corrosion Inhibition Characteristics of Azo Compounds on Carbon Steel under Sweet Conditions: Experimental and Theoretical Approaches. *ACS Omega*, 9(17), pp. 18932-18945.
- [3] Saad S T [2024]: Synthesis, characterization and theoretical aspects of copper and zinc divalent ion complexes with azo dye derived from 4, 5-diphenylimidazole. *Bulletin of the Chemical Society of Ethiopia*, 38(2), pp. 313-323.
- [4] Drommi M, Rulmont C, Esmieu C, & Hureau C. [2021]: Hybrid Bis-Histidine Phenanthroline-Based Ligands to Lessen A $\beta$ -Bound Cu ROS Production: An Illustration of Cu(I) Significance. *Molecules*, 26(24), p. 7630.
- [5] Moro J, Tomé D, Schmidely P, Demersay T C, & Azzout-Marniche D. [2020]: Histidine: A Systematic Review on Metabolism and Physiological Effects in Human and Different Animal Species. *Nutrients*, 12(5), p. 1414.
- [6] Rose W C. [1957]: The amino acid requirements of adult man. *Nutrition Abstracts and Reviews*, 27(3), pp. 631-647.
- [7] Wu G. [2009]: Amino acids: metabolism, functions, and nutrition. *Amino Acids*, 37(1), pp. 1-17.
- [8] Farhana M , Nazmun N, & Fahmida S A . [2025]: Synthesis, Characterization and complexation of Schiff base ligand p-anisalcefuroxime with Cu<sup>2+</sup> and Fe<sup>2+</sup> ions; antimicrobial and docking analysis with PBP2xto , *Mediterr J Pharm Pharm Sci*. 5 (1),pp. 48-64 .
- [9] Zingel V, Leschke C, & Schunack W. [1995]: "Developments in histamine H1-receptor agonists," in *Progress in Drug Research / Fortschritte der Arzneimittelforschung / Progrès des recherches pharmaceutiques*, E. Jucker Ed. Basel: Birkhäuser Basel, 1995, ch. 2, pp. 49-85.

- [10] Kopple J D, & Swendseid M E. [1975]: Evidence that histidine is an essential amino acid in normal and chronically uremic man, *The Journal of Clinical Investigation*, 55(5), pp. 881-891.
- [11] Katie W A, & Hadi M A. [2023]: Synthesis, Characterization and Biological Screening Study of Some New Mixed Ligand Complexes with Pt(II) Complex. *Uttar Pradesh Journal of Zoology*, 44(7), PP. 16-31.
- [12] Jasim E J. [2022]: Synthesis, characterization of some transition metal complexes with new ligands derived from azo and azo-schiff base and study the biological activity of gold (III) complexes . Ph.D. Chemistry Department, College of Science , Univirersity of kufa .
- [13] Ward H A, Musa T M, & Nasif Z N. [2022]: Synthesis and characterization of some transition metals complexes with new ligand azo imidazole derivative, *Al-Mustansiriyah Journal of Science*, 33(2), pp. 31-38.
- [14] Witwit I N, Mubarak H M, Ibrahim R A, & Majeed M. M. [2024]: Synthesis, coordination study, and anti-microbial ability of new mixed-ligand complexes derivatized from azo imidazole, and 1, 10-phenanthroline, *Microbial Biosystems*, 9(2), pp. 19-29.
- [15] Jawad S H. & Al-Adilee K J. [2023]: Synthesis, spectroscopic characterization and biological activities as an anticancer and antioxidant of the Pd(II) and Pt(IV) complexes with a new azo dye ligand derived from 5-methyl imidazole, *Journal of Molecular Structure*, 1277(April), p. 134846.
- [16] Mahdy A R E, Abu Ali O A, Serag W M, Fayad E, Elshaarawy R F M, & Gad E M. [2022]: Synthesis, characterization, and biological activity of Co(II) and Zn(II) complexes of imidazoles-based azo-functionalized Schiff bases, *Journal of Molecular Structure*, 1259(July), p. 132726.
- [17] Ashoor L S , Rawa'a A M , & Al-Shemary R K R. [2021]: Applications of biological of Azo-Schiff base ligand and its metal complexes and: A review; *MJPS*. 8, (1).
- [18] Chavan S M , Rathod N V, Khadse R E , Ghugare C D, Jadhao J S , Kubade A V , Thakare P S, & Patil A B. [2024]: Spectrophotometric Complexation Study of 8-Hydroxyquinoline Based AZO Dye with Pb(II) Metal ION and their Antimicrobial Activities. *Indian Journal of Advances in Chemical Science*, 12(3), pp. 197-203.

- [19] Vaidya V V [2023]: The effects of heavy metal contamination on antioxidant enzyme activity and oxidative stress in the earthworm *Perionyx excavates*. *Uttar Pradesh Journal of Zoology*, 44(3), pp. 59–65.
- [20] Maliyappa M R, &Keshavayya J. [2022]: Cu(II), Co(II), Ni(II), Zn(II) and Cd(II) complexes of novel azo ligand 6-hydroxy-4 methyl-2 oxo-5-[(4,5,6,7-tetrahydro-1,3-benzothiazol-2-yl)diazenyl]-1,2-dihydropyridine 3-carbonitrile as potential biological agents: synthesis and spectroscopic characterization. *Chemical Papers*, 76(6), pp. 3485-3498.
- [21] Obaid S M H, Jarad A J, &Al-Hamdani A A Salih [2020]: Synthesis, Characterization and Biological Activity of Mixed Ligand Metal Salts Complexes with Various Ligands. *Journal of Physics: Conference Series*, 1660(1), p. 012028.
- [22] Hasan H A. [2021]: Synthesis And Characterization Of Fluorescent Schiff Bases And Their Metal Complexes From 9-Anthracenecarboxaldehy. *Systematic Reviews in Pharmacy*, 12(1), pp. 306-314.
- [23] Sawant A M, Sunder A V, Vamkudoth K R, Ramasamy S, & Pundle A. [2020]: Process Development for 6-Aminopenicillanic Acid Production Using Lentikats-Encapsulated *Escherichia coli* Cells Expressing Penicillin V Acylase. *ACS Omega*, 5(45), pp. 28972-28976.
- [24] Shekhany B , Ozer F, Aytar E, Bradosty S W , Boyraz M U, Gurol A O , Shaikh F K, & Suzergoz F. [2023]: Anticancer Effects of Heterocyclic Schiff Base Ligands and Their Metal Complexes on Leukemia Cells. *Indian Journal of Pharmaceutical Sciences*, 85(4), pp. 953-961.
- [25] Saad F A, El-Ghamry H A, Kassem M A, & Khedr A M. [2019]: Nano-synthesis, Biological Efficiency and DNA Binding Affinity of New Homobinuclear Metal Complexes with Sulfa Azo Dye Based Ligand for Further Pharmaceutical Applications. *Journal of Inorganic and Organometallic Polymers and Materials*, 29(4), pp. 1337-1348.